Actual Antenna Radiation Pattern Measurements in Reverberation Chamber

Miguel Á. García-Fernández[1], Guillaume Andrieu[1], Cyril Decroze[1], and David Carsenat[1]*

[1]Wave and Associated Systems (OSA) Department, XLIM Research Institute, UMR CNRS nº7252, University of Limoges, 123 avenue Albert Thomas, 87060 Limoges Cedex, France

miguel-angel.garcia-fernandez@xlim.fr, guillaume.andrieu@xlim.fr, cyril.decroze@xlim.fr, david.carsenat@xlim.fr

Abstract

A reverberation chamber (RC) is an electrically large, highly conductive resonant enclosure used as test facility for radiated emissions and immunity measurements on electronic devices. In current literature, it is commonly stated that antenna radiation patterns cannot be measured, if needed, in RC. On the contrary, in this contribution, a novel technique that allows for the first time to perform actual antenna radiation pattern measurements in RC is presented. In order to demonstrate its validity, the radiation pattern for both E- and H- planes of a horn antenna has been measured in an RC at 10 GHz, in X band, and compared to the ones obtained in anechoic chamber, being the results in good agreement.

1. Introduction

For immunity measurements and radiated emissions on electronic devices, reverberation chambers (RC's) are the typically used test facilities. They are basically electrically large, highly conductive resonant cavities, wherein each resonant mode excited can be expanded in a certain number of plane waves incident from different angles, their actual number depending on the geometry of the cavity (e.g., eight plane waves for an empty rectangular cavity, but a potentially infinite number of plane waves is conjectured in chaotic geometries), except when the loading of the RC is so heavy that the actual resonances vanish [1]. In addition, if we assume that every power spectral density measurement is performed with the same antennas present within the RC, the average power received by an antenna will be independent of its gain, directivity or equivalent area [2].

RC's have been proposed to 3GPP in Technical Report 37.976 [3] as one of the candidate methodologies for conformance testing of Multiple-Input-Multiple-Output (MIMO) Over-The-Air (OTA) performance. Nevertheless, based on currently available information, the same Technical Report states that antenna radiation patterns cannot be measured, if needed, with this candidate methodology based on RC. This is mainly because an RC emulates a rich isotropic multipath (RIMP) environment, and thus their angles-of-arrival (AoA) follow a uniform distribution over all directions in space, causing any measured figure of merit to be statistically independent of the orientation of the antenna under test (AUT) [4]. This is the opposite extreme of the pure line-of-sight (LOS) environment emulated in anechoic chamber (AC), being therefore difficult to distinguish a unique LOS component among all other non-line-of-sight (NLOS) multipath components inside an RC, in order to evaluate the radiation pattern of an AUT.

On the contrary, in this contribution, a novel technique that allows for the first time to perform actual antenna radiation pattern measurements in RC is presented. The technique makes use of plane wave decomposition and a spatial Doppler analysis, moving the AUT in order to obtain the Doppler power spectral density and, eventually, the AUT radiation pattern. In order to support the validity of this novel technique, the radiation pattern of a horn antenna has been measured at 10 GHz, in X band, for both E- and H- planes, and compared to the ones obtained in AC, being the results in good agreement.

2. Measurement Methodology

Let us consider a transmitting AUT and a fixed receiving antenna in LOS inside an RC. Let us also define a set of N points along this LOS as p_n, with $n = 1, \ldots, N$, and the AUT initial orientation (θ_0, φ_0) in spherical coordinates. When the receiving antenna is fixed and the transmitting AUT is rotated through angles $(\Delta\theta, \Delta\varphi)$ with respect to its initial orientation, the transmitted power LOS component is in direct variation to the AUT radiation pattern $G(\theta, \varphi)$, with $\theta = \theta_0 - \Delta\theta$, $\varphi = \varphi_0 - \Delta\varphi$. Thus, in order to measure this AUT radiation pattern $G(\theta, \varphi)$, it is essential to distinguish the LOS component of the channel transfer function $H(f, t)$ from all other NLOS multipath components. Likewise, this channel transfer function $H(f, t)$ is equivalent to the S-parameter $S_{21}(f, t)$ measured with a vector network analyzer

978-1-4673-5225-3/14/$31.00 ©2014 IEEE

(VNA) under stationary conditions, i.e., when no object is moving inside the RC, at a constant time t with respect to the fading time-scale, as shown in [5]–[7]. Then, in order to distinguish the corresponding LOS component of the S-parameter $S_{21}(f, t)$ for certain rotation angles $(\Delta\theta, \Delta\varphi)$, stationary measurements can be repeated locating the transmitting AUT at the different fixed positions p_n (i.e, the above-mentioned points along the original LOS between both the transmitting AUT and the fixed receiving antenna), with $n = 1, \ldots, N$, while maintaining the same rotation angles $(\Delta\theta, \Delta\varphi)$.

Although each of these S-parameters are measured under stationary conditions without Doppler frequency shift, we can readily obtain the time varying S-parameter $S_{21}(f, t)$ by linking the discrete samples $S_{21}(f, t_n)$ using $t_n = t_{n-1} + \Delta t$, where Δt not only accounts for the time needed to displace the transmitting AUT between two consecutive positions, p_{n-1} and p_n, at the corresponding speed, but also for the time needed to stabilize the AUT after each movement and the time needed by the VNA to acquire the S-parameter data. Using this relation, the discrete Fourier transform of the samples $H(f, t_n) = S_{21}(f, t_n)$ can be evaluated, and thus the Doppler power spectral density can finally be obtained using [8, Eq. 5]. Since the collected S-parameter $S_{21}(f, t_n)$ constitutes a discrete function, the Doppler power spectral density can then be expressed as

$$D_H\left(f,\xi\right)=\left|\sum_{n=1}^{N} S_{21}\left(f,t_n\right)\exp(-j2\pi\xi t_n)\right|^2 . \tag{1}$$

For clarity purposes, and in order to be independent of the time Δt elapsed between two consecutive stationary measurements, let us consider the plane wave decomposition of the modes excited in the RC for a certain frequency f. The spatial frequency v of a plane wave can then be defined as how often two points with the same phase are found per unit of distance. As illustrated in Fig. 1, the value of the spatial frequency v will be different depending on the direction it is evaluated, and since the receiving antenna is fixed in position and angle, this value will depend on the AoA of the plane wave. Thus, the spatial frequency v will reach its maximum possible value $v_{max} = 1 / \lambda$ when the plane wave is propagating along the LOS between the transmitting AUT and the fixed receiving antenna. However, when the AoA of the plane wave differs from the LOS direction in an angle α, it is easy to see that the spatial frequency v will then result in a lower value, that is, $v = \cos(\alpha) / \lambda = \cos(\alpha)\, v_{max} < v_{max}$

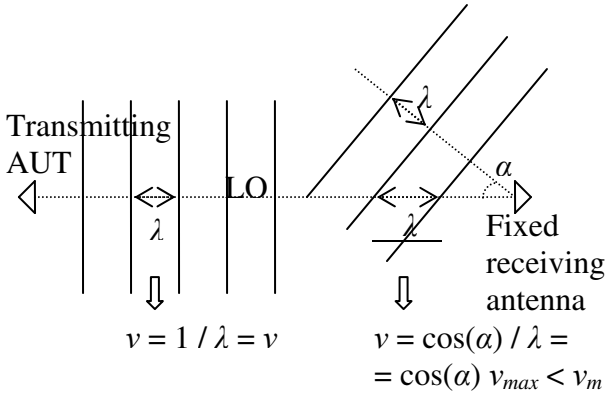

Fig. 1. Different spatial frequencies v for different plane wave AoA's.

As the discrete samples $H(f, t_n) = S_{21}(f, t_n)$ are measured for each corresponding p_n position, and also for each rotation angles $(\Delta\theta, \Delta\varphi)$, they can be rewritten as $S_{21}(f, p_n, \theta, \varphi)$ by linking directly each measurement time t_n with its corresponding transmitting AUT position p_n, and adding a dependence on the AUT orientation in $\theta = \theta_0 - \Delta\theta$ and $\varphi = \varphi_0 - \Delta\varphi$. Therefore, the Doppler power spectral density can be written in function of the spatial frequency v as

$$D_H\left(f,\nu,\theta,\varphi\right)=\left|\sum_{n=1}^{N} S_{21}\left(f,p_n,\theta,\varphi\right)\exp\left(-j2\pi\nu p_n\right)\right|^2 , \tag{2}$$

that is, as the squared absolute value of the discrete Fourier transform of the S-parameter $S_{21}(f, p_n, \theta, \varphi)$ with respect to the position p_n. Finally, since the transmitting AUT radiation pattern $G(\theta, \varphi)$ is in direct variation to the transmitted power LOS component, and also the spatial frequency v is maximized for the power received in the LOS direction, $G(\theta, \varphi)$ can therefore be calculated for a certain frequency f as

$$G\left(\theta,\varphi\right)=G\left(f,\theta,\varphi\right)\Big|_{f}=D_H\left(f,\nu_{\max},\theta,\varphi\right)=D_H\left(f,\frac{1}{\lambda},\theta,\varphi\right)=\left|\sum_{n=1}^{N} S_{21}\left(f,p_n,\theta,\varphi\right)\exp\left(-j2\pi\frac{1}{\lambda}p_n\right)\right|^2 . \tag{3}$$

3. Measured Results

In order to support the validity of the measurement methodology presented in the previous section, a horn antenna has been employed as transmitting AUT, and its radiation pattern has been evaluated inside an RC at a frequency of 10 GHz, in X band, for simplicity and without loss of generality. Likewise, an identical antenna is used as receiving antenna, which has been fixed in a tripod inside the RC.

In order to perform the stationary measurements required at N different points p_n along the LOS between the transmitting AUT and the fixed receiving antenna, a rail has been deployed inside the RC, and the AUT has been mounted on it. This rail counts with a linear axis to displace the AUT, and so the rail has been aligned with the mentioned LOS. A rotating axis is also present in the deployed rail, which is useful to change the AUT orientation in azimuth. This permits to calculate as many planes of the AUT radiation pattern as desired. For simplicity, the AUT radiation pattern has been measured for both the E- and H- planes. The RC where the measurements have been carried out, with dimensions 3.57 m × 2.46 m × 2.455 m, belongs to OSA Department at XLim Laboratory, and its inner view with all the mentioned elements deployed inside is shown in Fig. 2. Eventually, the S-parameter $S_{21}(f, p_n, \theta, \varphi)$ has been acquired with a VNA, moving the linear axis of the rail, and so the transmitting AUT, along a distance of $L = 1.8$ m, which correspond to 60 λ at 10 GHz, approximately. To get a correct estimate of the Doppler power spectral density, the distance between two consecutive AUT positions p_n must be small enough to satisfy Nyquist theorem, that is, smaller than $\lambda / 2$. In order to do so, $N = 163$ different p_n positions has been selected, equally spaced for simplicity, giving a separation between two consecutive positions of 0.37 λ approximately. The AUT has been rotated 180º with an angular step of 1º

The resulting radiation patterns are depicted in Fig. 3 and 4 for both E- and H- planes, respectively, and compared with the ones obtained in AC.

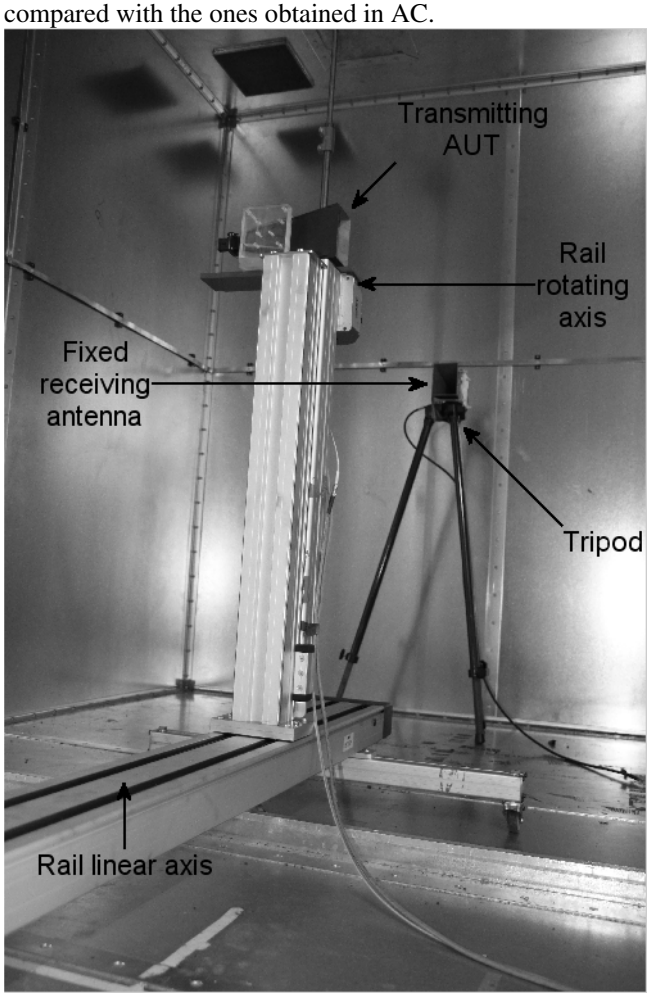

Fig. 2. Inner view of the RC and the deployed elements used in this study.

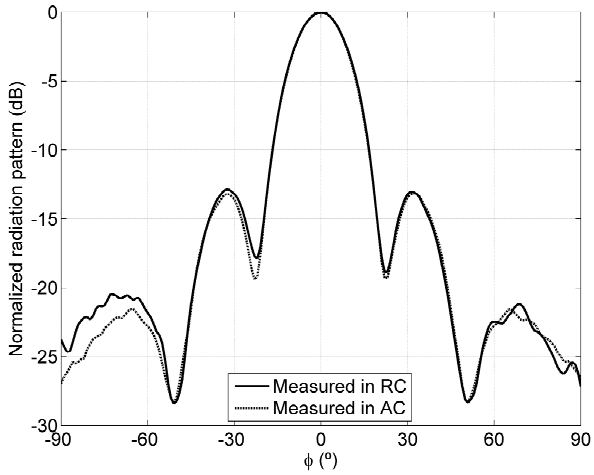

Fig. 3. AUT E-plane radiation pattern measured in RC and in AC.

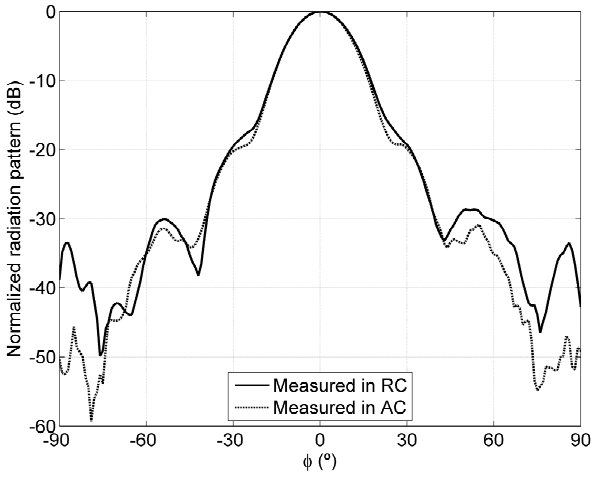

Fig. 4. AUT H-plane radiation pattern measured in RC and in AC.

As we can see, the radiation patterns retrieved from the measurements in RC through the novel methodology presented in this paper are almost coincident at the main and secondary lobes when compared to the radiation patterns measured in AC. Likewise, the maximum error made resulted to be lower than 3 dB for a dynamic range of 30 dB, except when the AUT is rotated ±90º.

Likewise, since the presented method required to perform measurements at N different points along the LOS between the transmitting AUT and the fixed receiving antenna, the measurement time resulted to be a few hours, that is, N times longer than measuring in AC. Thus, the presented method does not try to substitute an AC by an RC in order to perform radiation pattern measurements, but to provide a methodology that makes this kind of measurements possible in RC, against current knowledge, for the first time. In addition, the presented method could be useful when there is the need to perform antenna radiation pattern measurements, but there is no AC available to carry them out.

4. Conclusion

A novel methodology to perform actual antenna radiation pattern measurements in RC has been presented for the first time. Using this technique, a maximum error made lower than 3 dB has been achieved for a dynamic range of 30 dB, inside an RC with dimensions 3.57 m × 2.46 m × 2.455 m. The performance of the technique is dependent on the total distance *L* swept by the AUT, and thus, in order to improve the obtained results, it would be necessary to deploy a rail larger than the used along this study, or to work at a higher frequency.

However, even the obtained results could be improved in order to achieve accuracy comparable to the one attained in AC, this methodology presents, up to our knowledge, the best current option to perform this kind of measurements in RC. It could therefore be of special interest to define a methodology for measuring the radiated performance of multiple antenna reception and MIMO receivers, whose standardization is underway [3], [9].

References

1. K. Rosengren and P. S. Kildal, "Study of distributions of modes and plane waves in reverberation chambers for the characterization of antennas in a multipath environment," *Microwave and Optical Technology Letters*, vol. 30, no. 6, pp. 386–391, 20 Sep. 2001.

2. P. Corona, G. Latmiral, and E. Paolini, "Performance and Analysis of a Reverberating Enclosure with Variable Geometry," *IEEE Transactions on Electromagnetic Compatibility*, vol. EMC–22, no. 1, pp. 2–5, Feb. 1980.

3. 3rd Generation Partnership Project, "Measurement of radiated performance for Multiple Input Multiple Output (MIMO) and multi-antenna reception for High Speed Packet Access (HSPA) and LTE terminals (Release 11)," 3GPP Technical Report 37.976 v11.0.0, Mar. 2012.

4. P.-S. Kildal, C. Orlenius, and J. Carlsson, "OTA Testing in Multipath of Antennas and Wireless Devices With MIMO and OFDM," Proceedings of the IEEE, vol. 100, no. 7, pp. 2145–2157, Jul. 2012.

5. K. Karlsson, X. Chen, P.-S. Kildal, and J. Carlsson, "Doppler Spread in Reverberation Chamber Predicted From Measurements During Step-Wise Stationary Stirring," *IEEE Antennas and Wireless Propagation Letters*, vol. 9, pp 497–500, 2010.

6. S. J. Howard, K. Pahlavan, "Measurement and analysis of the indoor radio channel in the frequency domain," *IEEE Transactions on Instrumentation and Measurement*, vol. 39, no. 5, pp.751–755, Oct. 1990.

7. H. Hashemi, "Impulse response modeling of indoor radio propagation channels," *IEEE Journal on Selected Areas in Communications*, vol. 11, no. 7, pp.967–978, Sep. 1993.

8. M. Á. García-Fernández, D. Carsenat, and C. Decroze, "Antenna radiation pattern measurements in reverberation chamber using plane wave decomposition," *IEEE Trans. Antennas Propag.*, vol. 61, no. 10, pp. 5000–5007, Oct. 2013.

9. M. Á. García-Fernández, J. D. Sánchez-Heredia, A. M. Martínez-González, D. A. Sánchez-Hernández, and J. F. Valenzuela-Valdés, "Advances in Mode-Stirred Reverberation Chambers for Wireless Communication Performance Evaluation," *IEEE Communications Magazine*, vol. 49, no. 7, pp. 140–147, Jul. 2011.